RESEARCH ARTICLE

INTERNATIONAL RESEARCH JOURNAL OF MULTIDISCIPLINARY TECHNOVATION

Asian Research Association

DOI: 10.54392/irjmt25213

# Bio-efficacy of Polyethylene Glycol-coated Selenium Nanocomposite Synthesised using *Cocos nucifera* Haustorium against HepG2 Cell Line

**Y. Senthamaraikannan [a], V. Sundaram [a,*], R. Shanmugam [b]**

[a] Department of Biotechnology, Saveetha School of Engineering, Saveetha Institute of Medical and Technical Sciences, Chennai - 602105, Tamil Nadu, India

[b] Nanobiomedicine Lab, Centre for Global Health Research, Saveetha Medical College and Hospitals, Saveetha Institute of Medical and Technical Sciences, Chennai - 602105, Tamil Nadu, India

* Corresponding Author Email: hodbiotech.sse@saveetha.com

DOI: https://doi.org/10.54392/irjmt25213

Received: 18-11-2024; Revised: 05-03-2025; Accepted: 17-03-2025; Published: 30-03-2025

**Abstract:** The selenium-based nanoparticles (SeNP) are prepared by the amalgamation of *Cocos nucifera haustorium* (CNH) with sodium selenite. Further conjugating the synthesised CNH-SeNP with polyethylene glycol (PEG) to design haustorium-based selenium nanocomposite (CNH-SeNC). The work involves characterising and studying their bio-potency. Maximum absorption in UV-visible spectrum was at 315 nm and 305 nm for CNH-SeNP and CNH-SeNC. FT-IR affirms the involvement of functional groups of haustorium in the fabrication of CHH-SeNP and CNH-SeNC. SEM result conveys the spherical structure of the CNH-SeNP and the elongated oval shape of CNH-SeNC. EDX analysed the elemental proportion of CNH-SeNP and CNH-SeNC. X-ray diffraction pattern presents the amorphous form of CNH-SeNP with increased crystallisation in CNH-SeNC than that of CNH-SeNP. Regarding their antimicrobial activity, not much significant effect is seen. CNH-SeNP and CNH-SeNC comprised excellent antioxidant activity inferred by DPPH, ABTS, and $H_2O_2$ assays with the highest inhibition percentage of 84.67 ± 0.88 % and 86.24 ± 1.00 % through ABTS assays for CNH-SeNP and CNH-SeNC at 50 µg/mL. Egg albumin denaturation and HRBC assays showed potent anti-inflammatory properties. In HRBC, the inhibition of inflammation was equal to that of diclofenac sodium (positive control) 88.30 ± 0.66 %, followed by CNH-SeNC (87.77 ± 0.87 %) and CNH-SeNP (86.13 ± 0.83 %). Biocompatibility through brine shrimp lethality assay revealed that no toxicity was seen at low concentrations (10 µg/mL). Initially, mild toxicity was seen at 48 h for higher dosages (20 µg/mL) with viability 93.33±5.77% and 96.67±5.77% for CNH-SeNP and CNH-SeNC. The anticancer effect of CNH-SeNP and CNH-SeNC exhibited tremendous control of growth against HepG2 cells without affecting the normal cells with $IC_{50}$ values of 31.11 µg/mL and 24.41 µg/mL, respectively. Therefore, the study's outcome presents the advantages of green synthesis from *Cocos nucifera* haustorium and its conjugation with PEG providing their efficient pharmacological applications.

**Keywords:** Haustorium, Sodium selenite, Polyethylene glycol, Anticancer, Bio-compatibility

## 1. Introduction

Nanotechnology can revolutionise different arenas of science, especially agriculture and medicine [1]. Selenium (Se) is one among the essential micronutrients for maintaining the functions of thyroid hormone and immunity in humans. It is acquiring more interest among researchers because of its biomedical properties, including antioxidant properties [2]. The deficiency of Se causes cardiac, neuro-related, muscular, and other immune disorders. On the other hand, in-taking higher dosage may lead to adverse effects. So, it is highly required to consume the prescribed dose [3].

Generally, Se exists in selenite, selenate ions, selenoaminoacids, and selenoproteins. Selenium nanoparticles - SeNP have very less toxic effect than its organic and inorganic compounds. An alternative approach to synthesising the SeNP is through plant extracts; they offer an inexpensive, simple way of preparing the nanoparticles (NPs) without disturbing the environment. Further, it was stated that SeNP exhibits prominent antioxidant activity and antibacterial activity [4]. Various parts of *Cocos nucifera* are being used to synthesise numerous nanoparticles, including silver and gold [5, 6]. Another study used nettle leaves to synthesise SeNP, which possesses anticancer and

antimicrobial properties. They are effective against liver cancer (HepG2 cells) [7].

In certain studies, polyethene glycol (PEG), Polyvinylpyrrolidone (PVP) and various other polymers were capped on nanomaterials' surface, enhancing their biomedical properties. Incorporating PEG enhances the biocompatibility of respective nanomaterials [8]. Sesamol, an anticancer compound, was used along with Se-capped PEG for cancer treatment. They exhibited an increased efficacy in restraining the growth of anticancer cells, HepG2. Besides, from the results of flow cytometry analysis, it was witnessed that the fabricated nanomaterials caused more cell death when compared with that of either PEG or SeNP alone [9].

Like other parts of the *Cocos nucifera*, haustorium has recently gained interest among scientists due to its phytochemical content. The basal part of the embryo germinates to form the cotyledon called haustorium. The haustorium enlarges and occupies the liquid portion of the endosperm by 20-24 weeks after the onset of germination. Similar to coconut endosperm, the haustorium also possesses therapeutically important constituents such as resins, steroids, terpenoids, vitamins and minerals like potassium, magnesium and amino acids such as L-arginine [10, 11]. In addition to therapeutic applications, various parts of coconut fruit serve as precursors for the synthesis of nanomaterials [12].

The novelty of the present study lies in the utilisation of *Cocos nucifera* haustorium extract for selenium nanoparticle synthesis, highlighting its bio-medical potential and addressing the existing research gap in plant-based nanotechnology. None of the previous studies have utilised the haustorium of *Cocos nucifera* to synthesise SeNP. This study addresses the unexplored potential of *Cocos nucifera* haustorium as a biological reducing agent in the fabrication of selenium nanoparticles, which could provide a sustainable approach to nanomaterial synthesis. The hypothesis of the study has been explicitly stated; that to overcome the adverse effects and tedious methodology of chemical-based synthesis, green synthesis has been carried out. Accordingly, the primary aim of this study is to develop an eco-friendly, cost-effective synthesis of selenium nanoparticles (SeNP) using phytochemicals present in *Cocos nucifera* haustorium extract as natural bio-reductant. Further the study also focusses on the incorporation of PEG onto the surface of SeNP (CNH-SeNC) with aim to enhance the biomedical efficacy by improving the bio-availability and prolonged circulation time. The study is designed to explore the potential of these novel selenium nanomaterials (CNH-SENP and CNH-SeNC) for improved antioxidant, anti-inflammatory, anticancer efficacy against hepatocellular carcinoma (HepG2 liver cancer cells) without affecting normal cells indicating their potential application in targeted cancer therapies and biocompatibility.

Hence, the present study highlights the merits of sustainable approach of synthesising bio-compatible selenium nanomaterials by avoiding hazardous chemicals and minimising environmental impacts with enhanced therapeutic properties, providing a promising approach for future biomedical applications.

## 2. Materials and Methods

### 2.1 Reagents required

*Cocos nucifera* haustorium (CNH) was purchased from the local market in Chennai. Sodium selenite, PEG, 2, 2-diphenyl-1-picrylhydrazyl (DPPH), Potassium persulfate and 2, 2-azinobis (3-ethylbenzothiazoline-6-sulfonic acid (ABTS) were procured from SRL- Sisco Research Laboratories Chemicals. Muller Hinton agar and Rose Bengal agar (Hi-media), Hydrogen peroxide (MERCK), Ascorbic acid and Diclofenac sodium -Sigma-Aldrich, Dulbecco's Modified Eagle Medium (DMEM), Fetal Bovine Serum (FBS) were obtained from Gibco, (3-(4,5-dimethylthiazol-2-yl)-2,5-diphenyltetrazolium bromide) - MTT purchased from Invitrogen.

### *2.2 Synthesis and characterization*

#### *2.2.1 Synthesis of Cocos nucifera haustorium selenium nanoparticles (CNH-SeNP)*

The selenium nanoparticles were fabricated following the procedure done previously with minor modifications. A 100g of *Cocos nucifera* haustorium was homogenised using distilled water. It was heated (15-20 min), followed by filtration process through Whatman filter paper (No.1). The haustorium extract filtered was used as a bio-reductant, mixed dropwise to 30 mM sodium selenite in a ratio of 1:9 constantly, which was stirred continuously. Ultrasonication was carried out for 30 min at 50℃ and later kept in the shaker overnight at RT. Colour change and UV-visible readings were noted at different time intervals. The CNH-SeNP was lyophilised and stored for further biomedical studies [13, 14].

#### *2.2.2 Coating of Polyethylene glycol (PEG) on CNH-SeNP*

*Cocos nucifera* haustorium selenium nanocomposite (CNH-SeNC) was fabricated by coating CNH-SeNP with PEG following a slightly modified procedure from methods reported previously. 10 mL PEG was mixed to synthesised selenium nanoparticles 100 mL at appropriate temperature, maintained under constant stirring. The CNH-SeNC was allowed to dry in hot-air oven at 40°C, 10 hr; collected and stored. CNH-SeNC was characterised and evaluated for therapeutical potency [15].

#### *2.2.3 Characterisation studies of CNH-SeNP and CNH-SeNC*

UV-Visible spectrophotometer analysed absorption peaks of CNH-SeNP and CNH-SeNC (ESICO- model No. 3375) with wavelength ranging from 250-650 nm. Fourier transform infrared spectroscopy (FTIR) (BRUKER) analysed the functional groups in synthesised selenium nanoparticles and nanocomposite from 400 - 4000 $cm^{-1}$. SEM (scanning electron microscopy) (JEOL JSM IT-800) examined the structure along with their elemental composition by EDX (Energy dispersive X-ray) studies. The average diameter of CNH-SeNP and CNH-SeNC was calculated by Image J software. The crystallographic nature of CNH-SeNP and CNH-SeNC was analysed by D8-advance X-ray diffractometer (BRUKER, Germany).

### *2.3 Antimicrobial activity of CNH-SeNP and CNH-SeNC*

The microorganisms such as *Escherichia coli, Pseudomonas aeruginosa, Staphylococcus aureus, Enterococcus faecalis* were used for studying the antibacterial properties. *Candida albicans* is used in this procedure to study the antifungal activity. Cultures were obtained from the Department of Microbiology, Saveetha Medical College, Saveetha Institute of Medical and Technical Sciences, Thandalam, Chennai. Agar well diffusion technique determined the antimicrobial activity of CNH-SeNP and CNH-SeNC. Sample volumes (25 µg/mL, 50 µg/mL, 100 µg/mL), for positive control Cocos nucifera haustorium extract (25 µg/mL) in nanoparticle plates and CNH-SeNP (25 µg/mL) in nanocomposite plates were added to the corresponding wells. After incubating for a period of 24 h at 37 ºC, the diameter of inhibition zone was measured to analyse the sensitivity of microbes to CNH-SeNP and CNH-SeNC [16].

### 2.4 Antioxidant Assays

#### *2.4.1 DPPH Assay*

The scavenging capacity of CNH-SeNP and CNH-SeNC were estimated using DPPH activity slightly changed procedure from previous methods [17]. 1 mL of freshly prepared DPPH (20 µM) was combined with different aliquots (10-50 µg mL-1) of CNH-SeNP and CNH-SeNC. The prepared tubes were undisturbed for 30 min at RT in dark. Optical density (OD) at 517 nm was noted.

#### *2.4.2 ABTS Scavenging Activity*

ABTS cation scavenging activity was done with minor modifications in the previously reported methodology [18]. 7 mM ABTS and 2.45 mM potassium persulfate was combined and left at dark, 12-16 hr. The above solution OD was adjusted to 0.7 at 734 nm. The CNH-SeNP and CNH-SeNC (10-50 µg/mL) were added to 180 µL ABTS solution; after 6 min, this was placed in a 96-well microplate reader and quantified.

#### *2.4.3 $H_2O_2$ scavenging assay*

The hydrogen peroxide assay was performed with minor modifications in earlier method [19]. Dilutions (10-50 µg/mL) of CNH-SeNP and CNH-SeNC were measured and made up to 0.1 mL with 50mM phosphate buffer saline (pH 7.4). Following this, 0.9 mL of 2mM $H_2O_2$ reagent was taken. Vortex the above content, and after 10 min, optical density was noted at 230 nm.

Standard - Ascorbic acid (1 mg/mL) was used for all antioxidant assays.

### 2.5 Anti-Inflammation Assays

#### *2.5.1 Egg Albumin denaturation assay*

The anti-inflammation properties of the CNH-SeNP and CNH-SeNC were determined using an *in-vitro* egg albumin denaturation assay [20]. 0.2 mL of fresh egg albumin and 2.8 mL of PBS were combined. To this aliquot of CNH-SeNP and CNH-SeNC (10-50 µg/mL) were added, kept for 15 min at 37 °C, later at 70 °C, 5 min in the water bath, OD was quantified at 660 nm.

#### *2.5.2 Human RBC-Membrane stabilisation activity*

Efficiency of CNH-SeNP and CNH-SeNC to prevent the cell rupture by stabilising its membrane is inferred by HRBC assay [21]. A sterile centrifuge tubes with anti-coagulant were used to collect fresh blood sample. Human red blood cells (HRBC) were separated from the other components in the blood by centrifuging at RT 5 min at 3000 rpm. Discard the supernatant and wash the pellet (HRBC) by centrifugation, repeatedly for three times using normal saline. HRBC suspension of 10% (volume/volume) was obtained by suspending the pellet in 10 mM PBS (pH 7.4). Dilutions of the samples (CNH-SeNP and CNH-SeNC) 10-50 µg/mL, 0.5 mL of PBS buffer, 2 mL hyposaline and 0.5 mL suspended HRBC were taken together in centrifuge tubes, mixed slowly and left at 37 °C, 30 min. The above content was centrifuged at 3000 rpm, 3 min, RT. Using UV-visible spectrophotometer the supernatant's OD was observed at 560 nm.

The positive control used in anti-inflammatory assay was diclofenac sodium.

The inhibition percent for all assays was ascertained and analysed from the below equation

$$Inhibition\ (\%) = \left[\frac{Control\ OD\ -\ Sample\ OD}{Control\ OD}\right] * 100$$

Control OD= optical density of control; Sample OD = optical density of sample

## 2.6 Biocompatibility Analysis of CNH-SeNP and CNH-SeNC

The biocompatibility of the CNH-SeNP and CNH-SeNC synthesised from haustorium was studied using the brine shrimp lethality assay with minor modifications [22, 23].

### *2.6.1 Hatching of Artemia salina larvae*

In a rectangular jar, 3 litres of distilled water was taken; to this, 28 gm of NaCl was dissolved. Brine shrimp cysts were added to the above set-up, maintained at 22 – 29 °C with sufficient air supply and illumination for 24 - 48 h. The motile hatched nauplii were collected carefully and utilised for biocompatibility studies.

### *2.6.2 Lethality Assessment*

Freshly prepared saline water was taken in 6 well microtiter plates. To each well, 10 hatched nauplii were added. Different concentrations of CNH-SeNP and CNH-SeNC (5 $\mu gmL^{-1}$,10 $\mu gmL^{-1}$, 20 $\mu gmL^{-1}$, 40 $\mu gmL^{-1}$and 80 $\mu gmL^{-1}$) were used in the study. The number of dead and live nauplii in the plates after 24 h and 48h was noted. The rate of viability was assessed by the below equation,

$$\% \, viability = \left[\frac{number \; of \; alive \; nauplii}{total \; number \; of \; nauplii}\right] * 100$$

## 2.7 In-vitro toxicity and anti-cancer activity by MTT assay

### *2.7.1 Maintenance of cell culture*

Vero (African green monkey kidney normal epithelial cell line) and HepG2 (Human hepatocellular carcinoma epithelial cell line) were acquired from National Centre for Cell Sciences (NCCS), Pune, India. Cells in logarithmic phase were retained for the study. The DMEM with 10 % v/v of FBS (heat inactivated), 100 U/mL penicillin and 100 µg/mL streptomycin was used. The acquired cell lines were maintained at a temperature of 37 °C, and kept in CO2 (5%) in 95 percent air humidified incubator.

### *2.7.2 Assessment of cytotoxicity and anticancer activity*

The cytotoxicity and anticancer effect were evaluated using Vero and HepG2 cell line through MTT assay [24, 25]. 96-well micro-titre plates were taken in which cells were seeded (1 x $10^6$ cells/well). The incubated plates were maintained at 37 °C and 5 % $CO_2$ until they reached 80% confluency, with intermediate observation using a digital inverted microscope for any contamination or dead cells. Later, the medium was replaced by CNH-SeNP and CNH-SeNC (10 - 50 µg/mL) and incubated for 24 h. The structural modifications of samples in Vero and HepG2 were photographed in 20 X magnification under a digital inverted microscope. Control without a sample was also maintained. The cells in each well were washed using PBS (pH 7.4). 20 µL MTT reagent (5 mg/mL PBS) was added. The incubated plates are kept at 37 ºC for 2 h in the dark. Add 0.1 mL DMSO for dissolving the formed formazan crystals. These plates were quantified at 570 nm in 96-well plate reader. Viable cell percent was evaluated as follows:

$$\text{Viability of cells } (\%) = \left[\frac{Absorbance \; sample}{Absorbance \; control}\right] * 100$$

## 2.8 Statistical Analysis

All the experiments were performed as triplicates and the results are represented as mean ± standard deviation. The results were analysed by graph pad prism 5.0 using two-way ANOVA and Bonferroni post-test. The results are considered significant denoted by "*" when $p<0.001$.

# 3. Results

## 3.1 Synthesis of CNH-SeNP and CNH-SeNC

*Cocos nucifera* haustorium extract was added to sodium selenite (Figure 1a) for stabilising and reduction purposes. The change in colour to red from the colourless solution confirms the conversion of selenite to its elemental form ($Se^0$), which affirms the synthesis of CNH-SeNP (Figure 1b), thus showing the involvement of phytochemicals in the haustorium for the bio-synthesis. The formation of CNH-SeNC by coating PEG on CNH-SeNP is shown in Figure 1c.

## 3.2 Characterisation of CNH-SeNP and CNH-SeNC

### *3.2.1 UV-Visible spectrum*

The UV-visible analysis of synthesised CNH-SeNP and CNH-SeNC revealed the surface plasmon resonance excitation with maximum absorption spectrum at 315 nm (Figure 2a) and 305 nm (Figure 2b), indicating the reduction process resulting in reduction to elemental selenium, which might be due to involvement of *Cocos nucifera* haustorium's secondary metabolites.

### *3.2.2 FTIR spectroscopy*

FTIR spectra (Figure 3) showed multiple peaks at 3276 $cm^{-1}$ depicting strong vibrational O-H stretch, 2924.46 $cm^{-1}$ denoting C-H stretch with weak vibrations [11], 1584.72 $cm^{-1}$ corresponding to N-H bend amines, 1399 $cm^{-1}$ denoting stretch of C-C carbohydrates (glucose) [26], 1032.61 $cm^{-1}$ representing C-O stretch of secondary alcohol [27] and 922.75 $cm^{-1}$ indicating β-pyranose ring for CNH-SeNP [11].

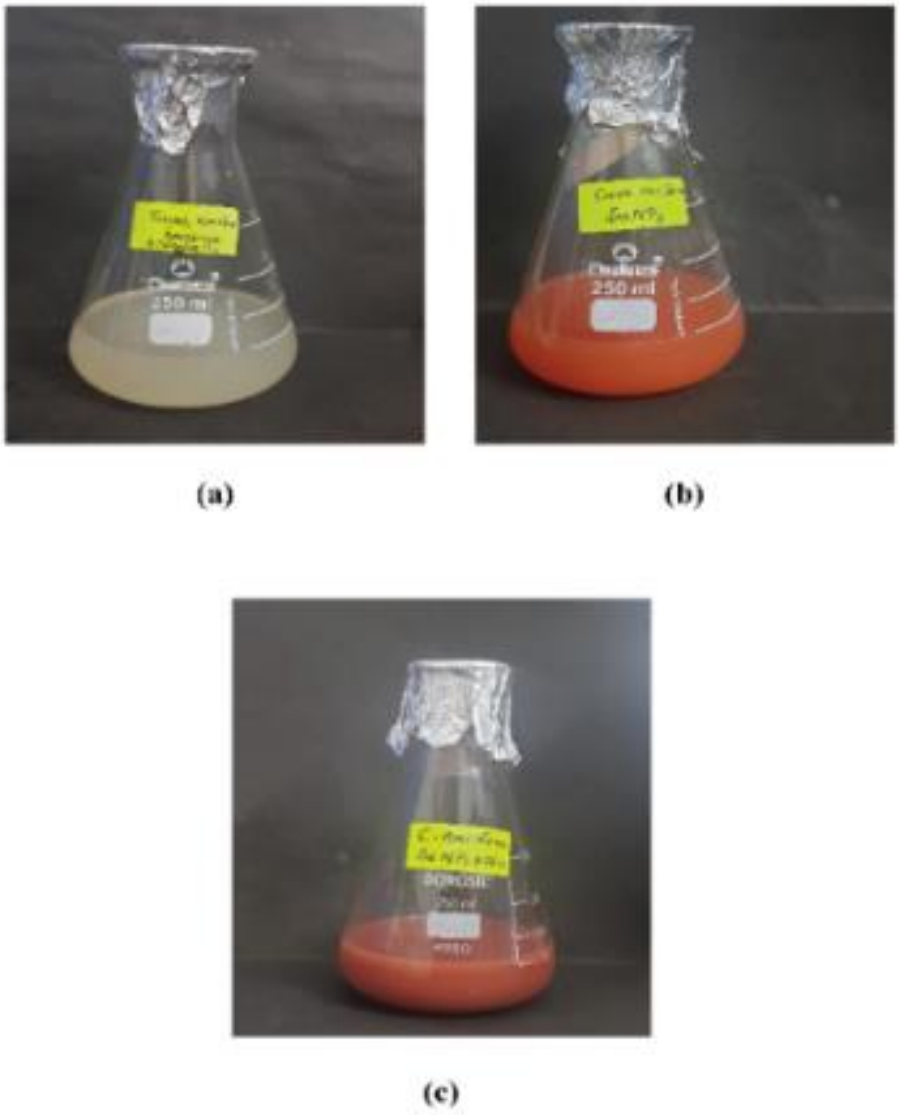


**Figure 1.** Synthesis a) *Cocos nucifera* Haustorium (CNH) extract with sodium selenite, **b)** CNH- SeNP **c)** CNH-SeNC

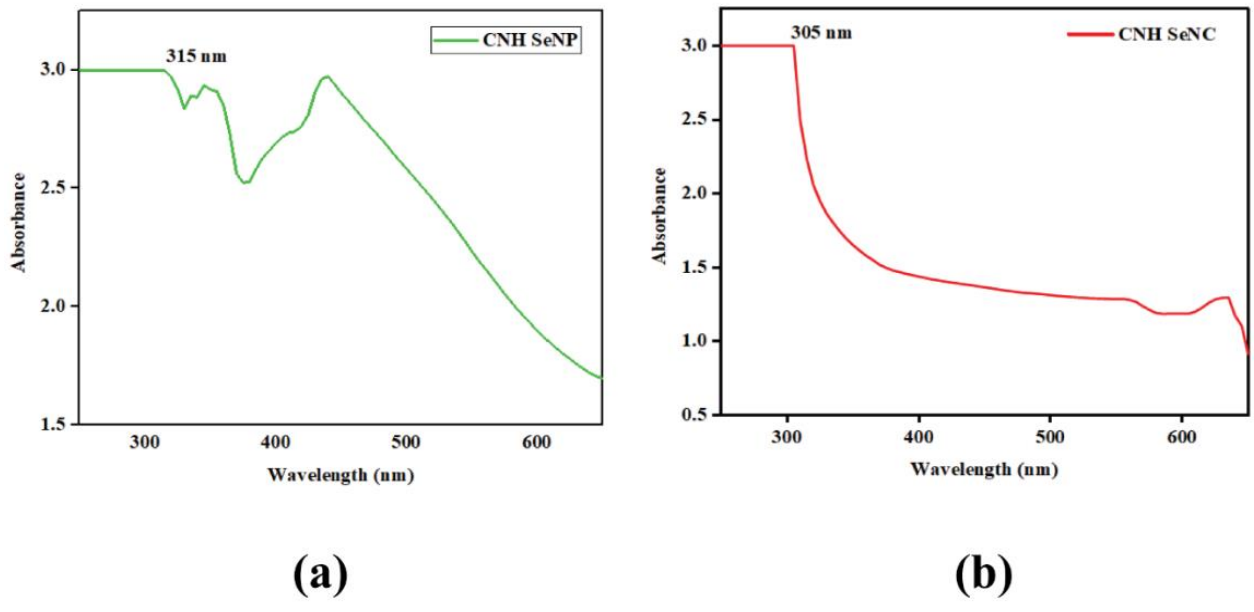


**Figure 2.** UV-Visible spectrum a) CNH-SeNP b) CNH-SeNC

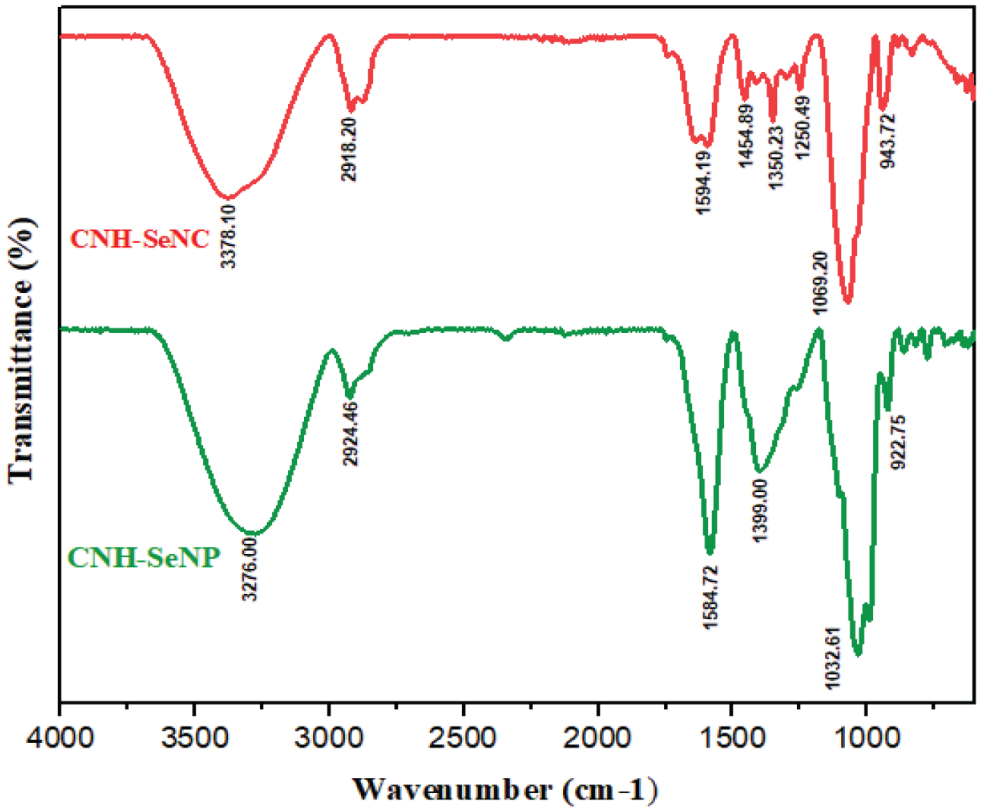


**Figure 3.** FTIR spectral analysis CNH-SeNP and CNH-SeNC

The IR spectra for CNH-SeNC exhibited absorption peaks at 3378.10 $cm^{-1}$ corresponds to strong O-H stretch vibrations [28], 2918.20 $cm^{-1}$ weak vibrational peak of C-H stretching [11], 1594.19 $cm^{-1}$ denoting N-H bend amines, 1454.89 $cm^{-1}$ indicating C-H bending methyl group, 1350.23 $cm^{-1}$ denotes symmetrical stretching of $CH_2$ group, 1250.49 $cm^{-1}$ corresponds to C-N stretch amines, 1069.20 $cm^{-1}$ denoting C-O stretch and 943.72 $cm^{-1}$ representing glycosidic linkage [29].

### 3.2.3. Morphological analysis and elemental composition by SEM-EDX

Surface morphology was analysed using SEM, which clearly depicts the spherical shape of CNH-SeNP, which appears to be well distributed, non-matrix embedded and mono-dispersive with an average diameter ranging from 90.71 nm (Figure 4a). CNH-SeNC has elongated oval morphology, embedded on core-matrix, less agglomerated with an average diameter of 502.16 nm (Figure 4b). Aluminum was used as the substrate material during the EDX analysis which is the reason for the existence of Al peak. The intensity peak in energy dispersive X-ray analysis of CNH-SeNP and CNH-SeNC at 1.37keV and 11.2keV indicates the selenium's presence in the samples there-by affirming the synthesis of selenium nanoparticles and nanocomposite. The weight percentage 5.6% and atomic percentage 1.1% for CNH-SeNP and that of CNH-SeNC is 13% and 2.5% respectively. The low sigma (σ) value 0.2 in both samples denote that Se is uniformly distributed and measured with high accuracy. The other elements present in CNH-SeNP are as follows carbon (C) and oxygen (O) with the weight percent 54.3%, 9.7% and atomic percent 71.5%, 9.6% respectively. Trace amount of Fe (0.4 wt%, atomic percent 0.1%) is also present. CNH-SeNC also contains carbon (C) and oxygen (O) with weight percentage 56.7%, 15.6% and atomic percentage 73.6%, 15.2% respectively. Mild traces (0.8 wt%, atomic percent-0.5%) of sodium (Na) are seen in CNH-SeNC. The sigma value of C (0.8) is very high which shows that it is not evenly distributed in the sample (Figure 4c and 4d).

### 3.2.4 XRD spectral pattern

The crystallinity of the synthesised CNH-SeNP and CNH-SeNC were assessed by XRD (Figure 5a and 5b). The broader peak reveals the amorphous nature of CNH-SeNP. The crystalline percentage of CNH-SeNP 9% has risen to 28.7 % in CNH-SeNC, depicted by the sharper peaks, which might be due to the attachment of PEG. The XRD analysis (JCPDS File No. 06-0362) depicts Bragg's peak with reflection planes at 42.55º (1 1 0) and 43.64 º (1 0 2) for CNH-SeNP and for CNH-SeNC were at 23.62 º (1 0 0), 29.84 º (1 0 1), 41.40 º (1 1 0), 43.69 º (1 0 2), 45.37 º (1 1 1), 51.88 º (2 0 1), 55.95 º (1 1 2), 61.6 º (1 0 3) and 65.29 º (2 1 0).

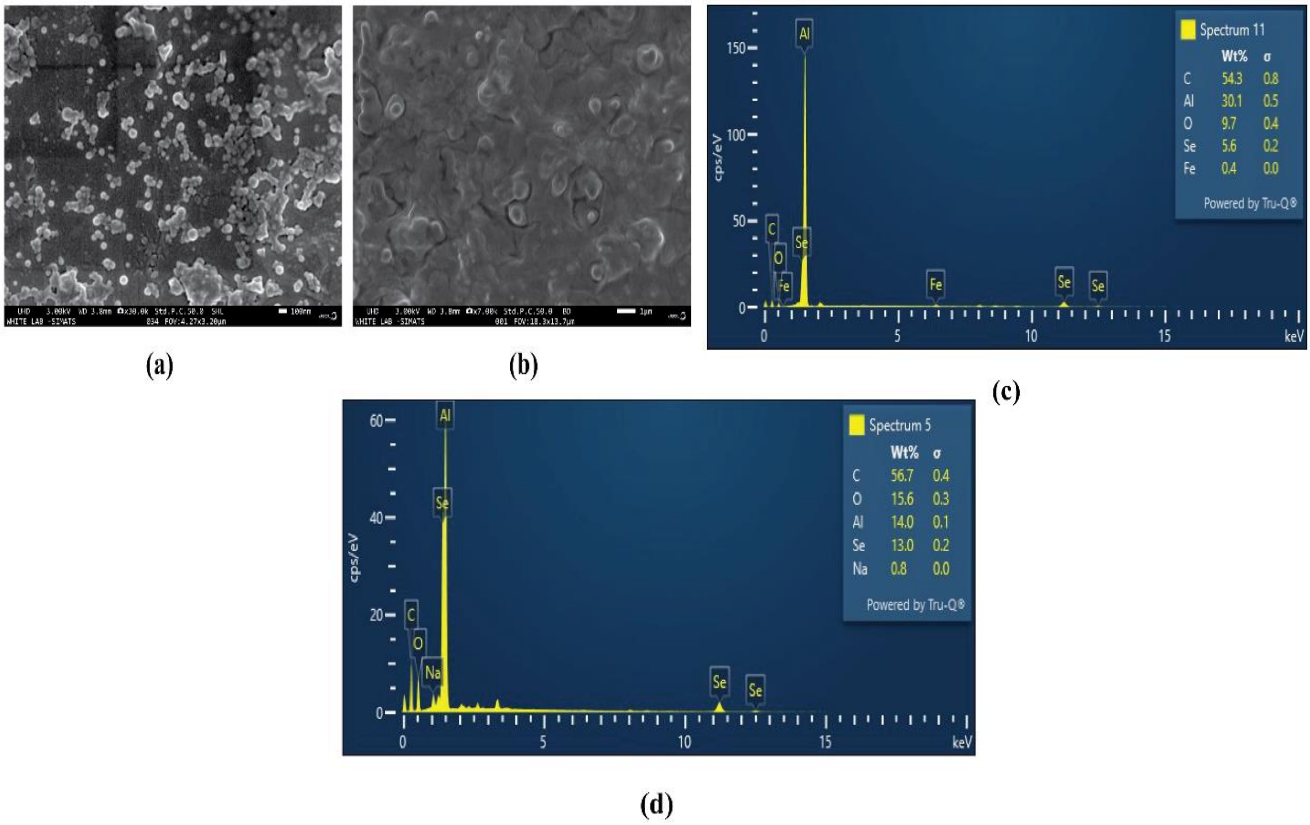


**Figure 4. a)** SEM image CNH-SeNP **b)** SEM image CNH-SeNC **c)** EDX CNH-SeNP **d)** EDX CNH-SeNC

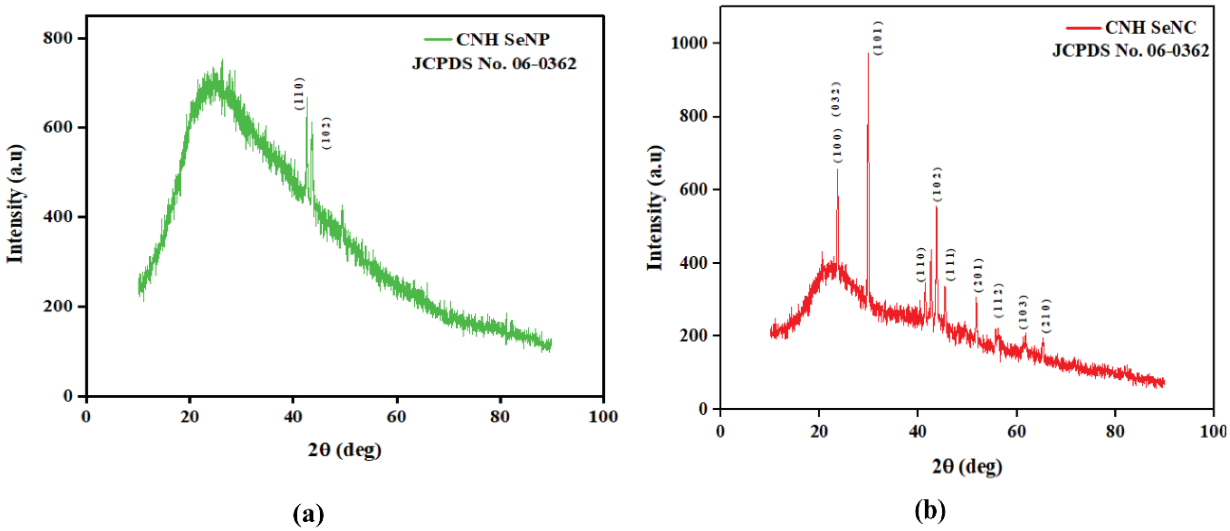


**Figure 5.** XRD spectral pattern **a)** CNH-SeNP **b)** CNH-SeNC

The 2-theta peak value at 23.62 º corresponding to the reflection plane (0 3 2) represents PEG.

### 3.3 Antimicrobial activity of CNH-SeNP and CNH-SeNC

The antibacterial activity of CNH-SeNP (Figure 6) and CNH-SeNC (Figure 7) had no significant effect against microbes *Escherichia coli, Pseudomonas aeruginosa, Staphylococcus aureus* and *Enterococcus faecalis* at 25 and 50 µg/mL. At 100 µg/mL, the inhibition zone was 13.0 ± 0.0 mm, 11.0±0.0 mm, 11.33 ± 0.58 mm, 11.33 ± 0.58 mm and 11.0 ± 0.0 mm, 10.67 ± 0.58 mm, 10.33 ± 0.58 mm, 11.33 ± 0.58 mm for CNH-SeNP and CNH-SeNC. Meanwhile, for *Candida albicans*, CNH-SeNC had minimal activity than CNH-SeNP, which had no activity. The zone of inhibition for CNH-SeNC at 25, 50, 100 µg/mL was 10.67 ± 0.58 mm, 11.0 ± 0.0 mm, 12.0 ± 1.0 mm.

## 3.4 Antioxidant potential

### *3.4.1 DPPH Assay*

The reduction of free radicals pertaining to CNH-SeNP and CNH-SeNC using DPPH assay can be inferred visually by the colour change from purple to pale purple or yellow. At 10 µg/mL, antioxidant activity exhibited by CNH-SeNP, CNH-SeNC and standard is 53.72 ± 0.88 %, 60.37 ± 0.73 %, 65.97 ± 1.36 %. The inhibition percentage of CNH-SeNP, CNH-SeNC, standard was found to be 80.72 ± 0.98 %, 87.08 ± 0.90 %, and 92.24 ± 0.79 % at 50 µg/mL. The sequestration of free radicals increases at sample's higher concentration. The percentage inhibition shows that CNH-SeNC has better antioxidant activity than CNH-SeNP. Figure 8a represents the results of DPPH activity.

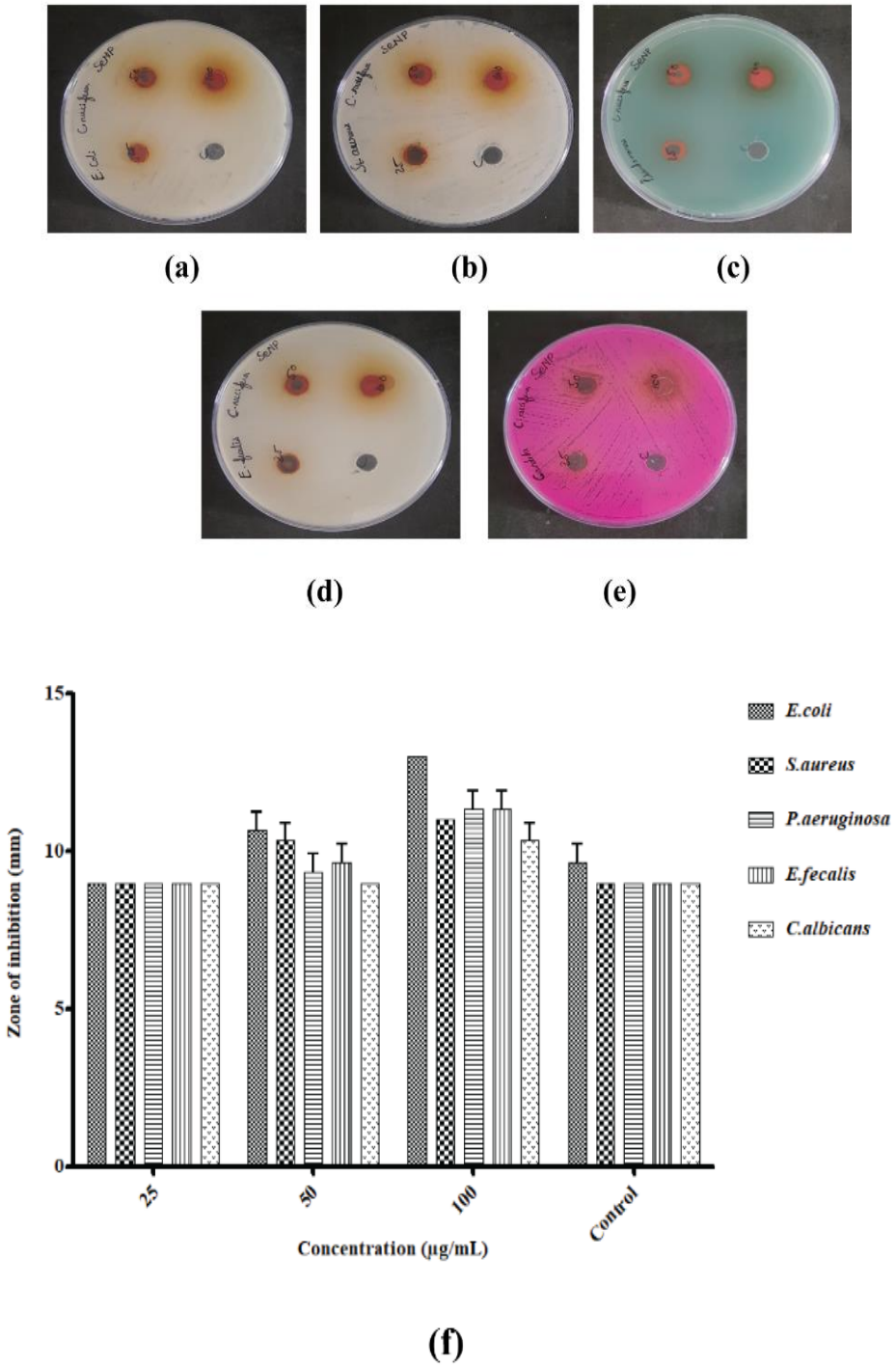


**Figure 6.** Antimicrobial activity of *Cocos nucifera* haustorium selenium nanoparticle, **a)** *Escherichia coli* **b)** *Staphylococcus aureus* **c)** *Pseudomonas aeruginosa* **d)** *Enterococcus faecalis* **e)** *Candida albicans* **f)** Graphical depiction of antimicrobial activity

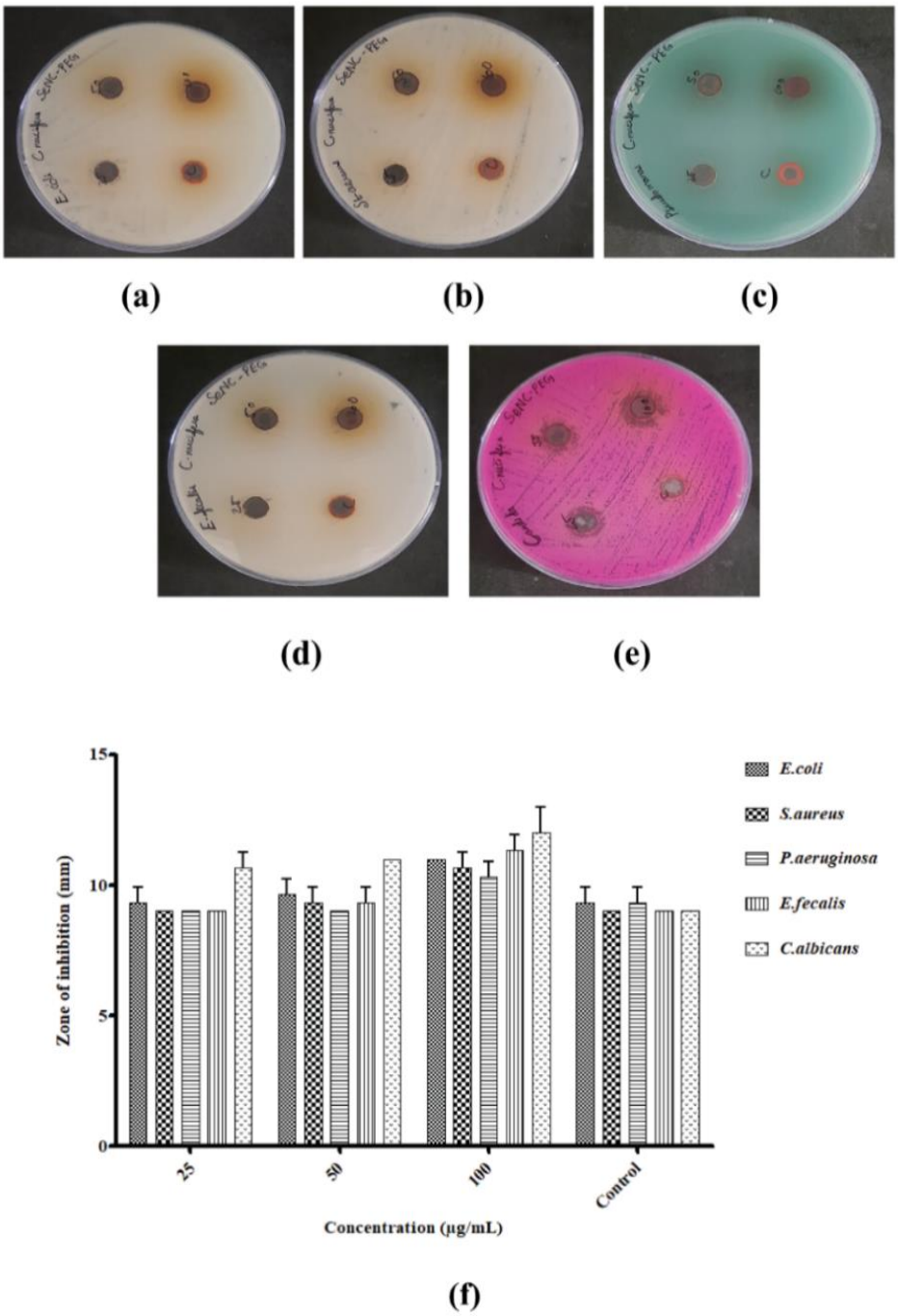


**Figure 7.** Antimicrobial activity of *Cocos nucifera haustorium* selenium nanocomposite **a)** *Escherichia coli* **b)** *Staphylococcus aureus* **c)** *Pseudomonas aeruginosa* d) *Enterococcus faecalis* **e)** *Candida albicans* **f)** Graphical depiction of antimicrobial activity

### *3.4.2 ABTS Scavenging Assay*

The conversion of blue-green to a colourless solution infers that the antioxidant content of the sample reduces the free radicals. ABTS assay revealed the percentage inhibition of CNH-SeNP and CNH-SeNC to be 84.67 ± 0.88 % and 86.24 ± 1.00 % for the concentration 50 µg/mL. The inhibition capacity of standard was found to be 90.62 ± 0.85 % at 50 µg/mL. At 10 µg/mL, the scavenging capacity was 59.95 ± 0.95 %, 65.37 ± 0.83 %, and 70.66 ± 0.81 % for CNH-SeNP, CNH-SeNC and standard, respectively. Above results infers that the antioxidant capacity of samples is directly proportional to sample concentration. ABTS scavenging activity is depicted in Figure 8b.

### *3.4.3 Hydrogen peroxide scavenging assay*

$H_2O2$ reduces to highly reactive redox radicals, causing damage to cells through oxidation. The scavenging percentage of CNH-SeNP and CNH-SeNC are found to be 47.79 ± 0.92 % and 49.18 ± 0.88 % at 10 µg/mL, the same at 50 µg/mL is 74.28 ± 0.86 % and 81.44 ± 0.90 %.

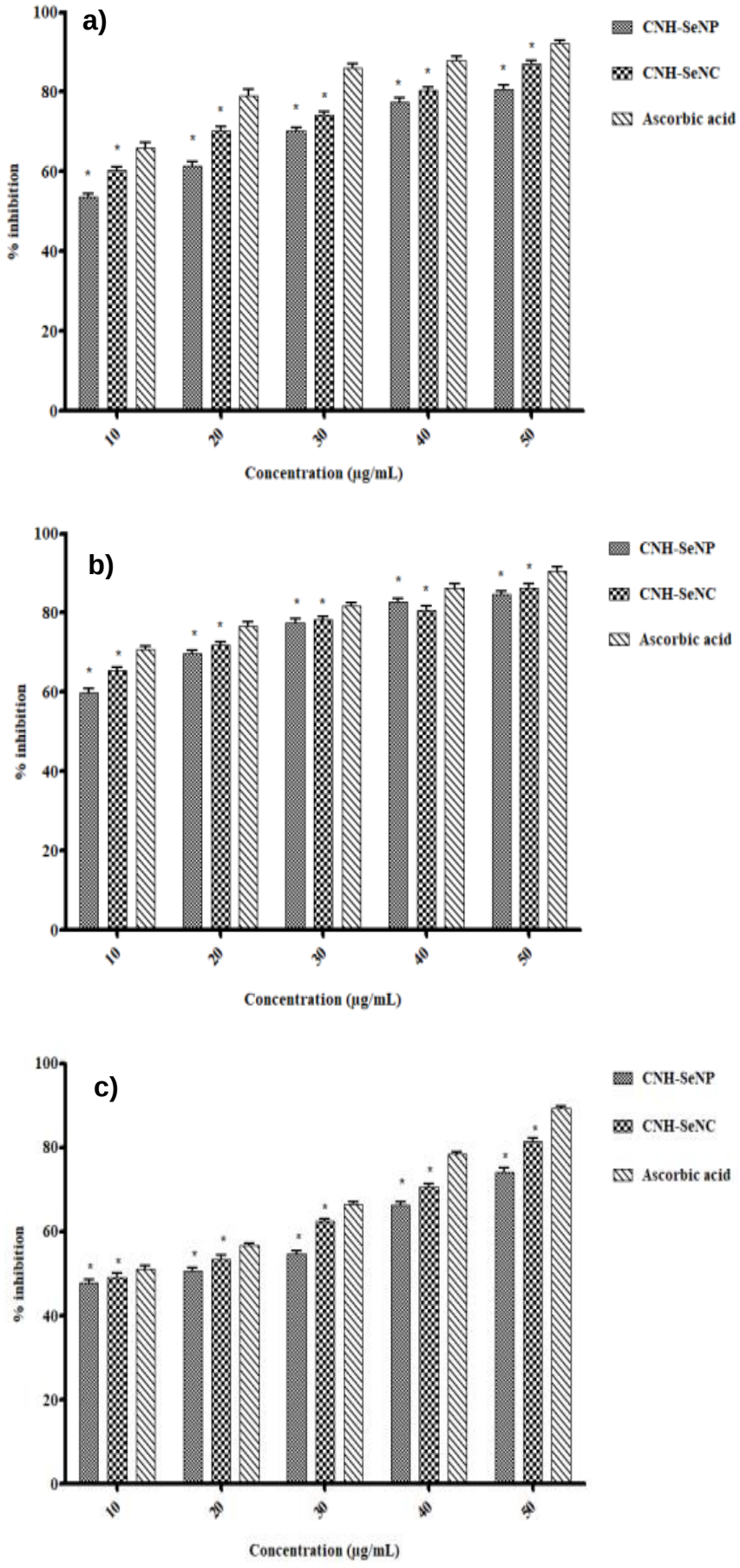


**Figure 8.** Antioxidant potential of CNH-SeNP and CNH-SeNC with standard (Ascorbic acid) a) DPPH assay b) ABTS activity c) Hydrogen peroxide assay

The inhibition percentage of ascorbic acid was 51.24 ± 0.70 % and 89.25 ± 0.61 % at 10 and 50 µg/mL. Figure 8c represents $H_2O_2$ scavenging assay.

## 3.5 Evaluation of Anti-inflammatory potency

### *3.5.1 Egg albumin denaturation assay*

Anti-inflammation potency of CNH-SeNP and CNH-SeNC were evaluated through egg albumin denaturation activity. The anti-inflammatory potency of CNH-SeNP and CNH-SeNC was measured to be 51.26 ± 0.85 % and 53.53 ± 0.97 % at 10 µg/mL, and that of diclofenac sodium at the same concentration was 55.38 ± 0.94 %. At 50 µg/mL, anti-inflammatory efficiency was 77.62 ± 0.86 %, 77.97 ± 0.94 % and 81.33 ± 0.95 % for CNH-SeNP, CNH-SeNC and diclofenac sodium. Figure 9a depicts the comparative anti-inflammatory effect of samples with that of diclofenac sodium (positive control).

### *3.5.2 Human RBC-Membrane stabilisation assay*

*In-vitro* anti-inflammatory activity revealed about the membrane stabilisation property of CNH-SeNP, and CNH-SeNC by HRBC assay. At 10 µg/mL CNH-SeNP, CNH-SeNC and positive control exhibited 56.35±0.85%, 57.14±0.94% and 58.33±0.77% activity. The anti-inflammatory effect of CNH-SeNP, CNH-SeNC and positive control is found to be 86.13±0.83%, 87.77±0.87%, 88.30±0.67% at 50 µg/mL. Figure 9b presents the anti-inflammatory effect of samples and positive control.

## 3.6 Biocompatibility property - *Brine shrimp lethality assessment*

To assess the biocompatibility of CNH-SeNP and CNH-SeNC, a brine shrimp lethality assay was conducted. The percentage viability of brine shrimp nauplii was noted for several sample concentrations, which reveals that the viability of nauplii decreased with an increase in concentration. Figure 10 depicts the percentage of live nauplii for CNH-SeNP and CNH-SeNC. A well without a sample was maintained as a control, and it had 100% live nauplii.

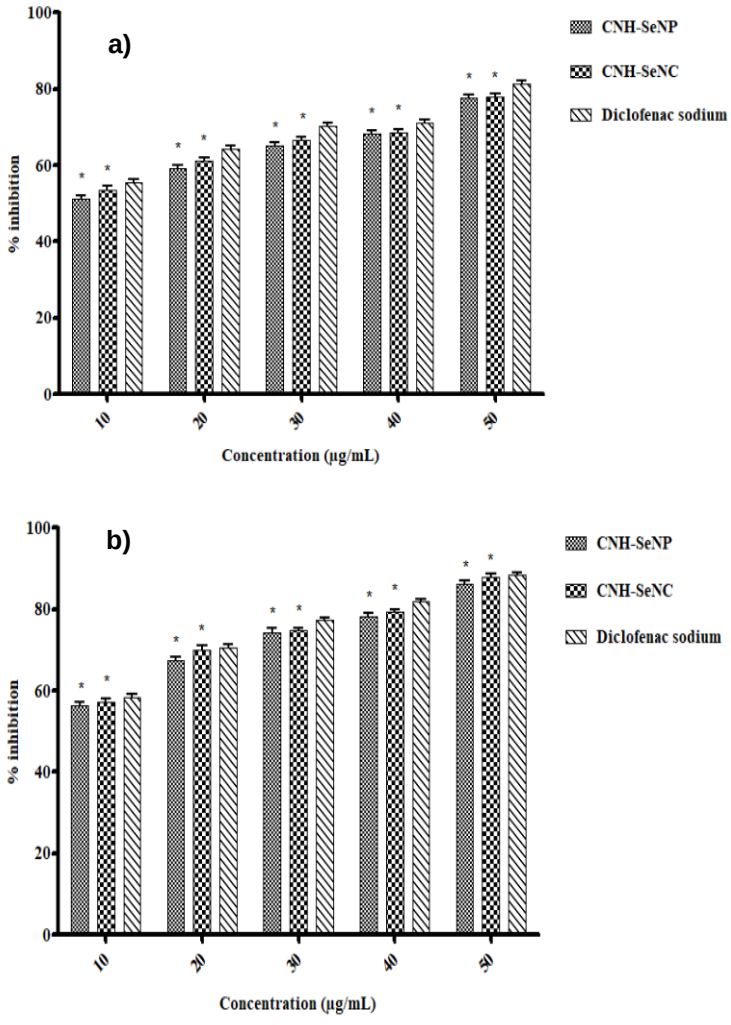


**Figure 9.** Anti-inflammatory potency of CNH-SeNP and CNH-SeNC with Diclofenac sodium (positive control) a) Egg albumin denaturation assay **b)** HRBC assay

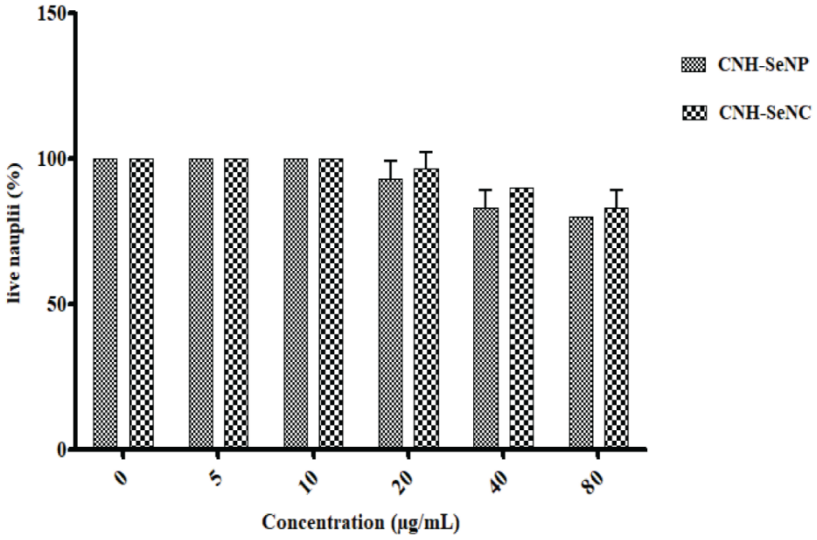


**Figure 10.** Brine shrimp lethality activity depicting the viability per cent of nauplii after treating 48 h with CNH-SeNP and CNH-SeNC

All brine shrimp nauplii were motile after 24 h of treatment, and they showed 100% viability. After treatment for 48 h, samples did not exhibit toxic effects at lower concentrations up to 10 µg/mL. Mild toxicity was observed at higher concentrations of 20 µg/mL, 40 µg/mL and 80 µg/mL for CNH-SeNC with viability percentages 96.67 ± 5.77 %, 90.00 ± 0.00 %, 83.33 ± 5.77 %. The percentage of live nauplii observed for CNH-SeNP at 20 µg/mL, 40 µg/mL, and 80 µg/mL were 93.33 ± 5.77 %, 83.33 ± 5.77 % and 80.00 ± 0.00 %.

### *3.7 Cytotoxic effect and anticancer activity*

The cytotoxicity of CNH-SeNP and CNH-SeNC was determined using an MTT assay on *Vero* cell line. Even at 50 µg/mL, the percent of cells viable were 85.78 ± 0.36 % and 89.66 ± 0.65 % for CNH-SeNP and CNH-SeNC, respectively. The anticancer property was done against hepatocellular carcinoma on HepG2 cell lines. The samples CNH-SeNP and CNH-SeNC expressed potent anticancer effects showing lower viable percentages, 18.51 ± 0.54 % and 8.21 ± 0.62 % at 50 µg/mL compared to 93.11 ± 0.88 % and 81.13 ± 0.61 % at 10 µg/mL. Figure 11a and Figure 11b presents the cell viability percent of CNH-SeNP and CNH-SeNC along with their $IC_{50}$ value.

Both CNH-SeNP and CNH-SeNC did not cause much significant morphological change in the *Vero* cell line (Figure 12a - 12c). It is clearly evident that CNH-SeNP and CNH-SeNC lead to remarkable changes in the morphology of the HepG2 cell line when compared to the control without any sample (Figure 12d - 12f). After treatment, the liver cancer cell line has resulted in shrinkage and become round in shape. Cell viability was extremely reduced as concentration increased.

## 4. Discussion

Universally, the death caused by cancer is increasingly widely attributed to our lifestyle changes, food habits and our surroundings. Though there are many synthetic drugs, the adverse effects of these drugs on healthy cells lead us to do more research on the alternate approach to combat the diseased condition [30]. The study's fundamental objective is synthesising selenium nanoparticles from the haustorium of *Cocos nucifera*. The preparation of *Cocos nucifera* haustorium extract by heating 15-20 minutes increases the solubility of bio-molecules without degradation of bio-molecules as prolonged heating by denature the phytocompounds. The process of ultrasonication for 30 minutes at the temperature 50°C improvise the uniform mixing, preventing agglomeration and increases the dispersion of nanoparticles by enhancing the reduction process by haustorium extract. The higher temperatures would degrade the bio-molecules of the haustorium extract so moderate temperature of 50°C was maintained during ultrasonication. The duration of 30 minutes is sufficient for the formation of nanoparticles by limiting the use of more energy. Overnight incubation at room temperature in shaker ensures the completion of the reduction process and stabilisation of nanomaterials. The concentration of the precursor was chosen based on the earlier study [14].

The colour changes from colourless to red [31], which is attributed to a reduction of sodium selenite to selenium ($Se^0$) by the reduction process catalysed via metabolites present in haustorium. A similar colour change was seen for SeNP synthesised from *Melia azedarach* leaves using sodium selenite salt [32].

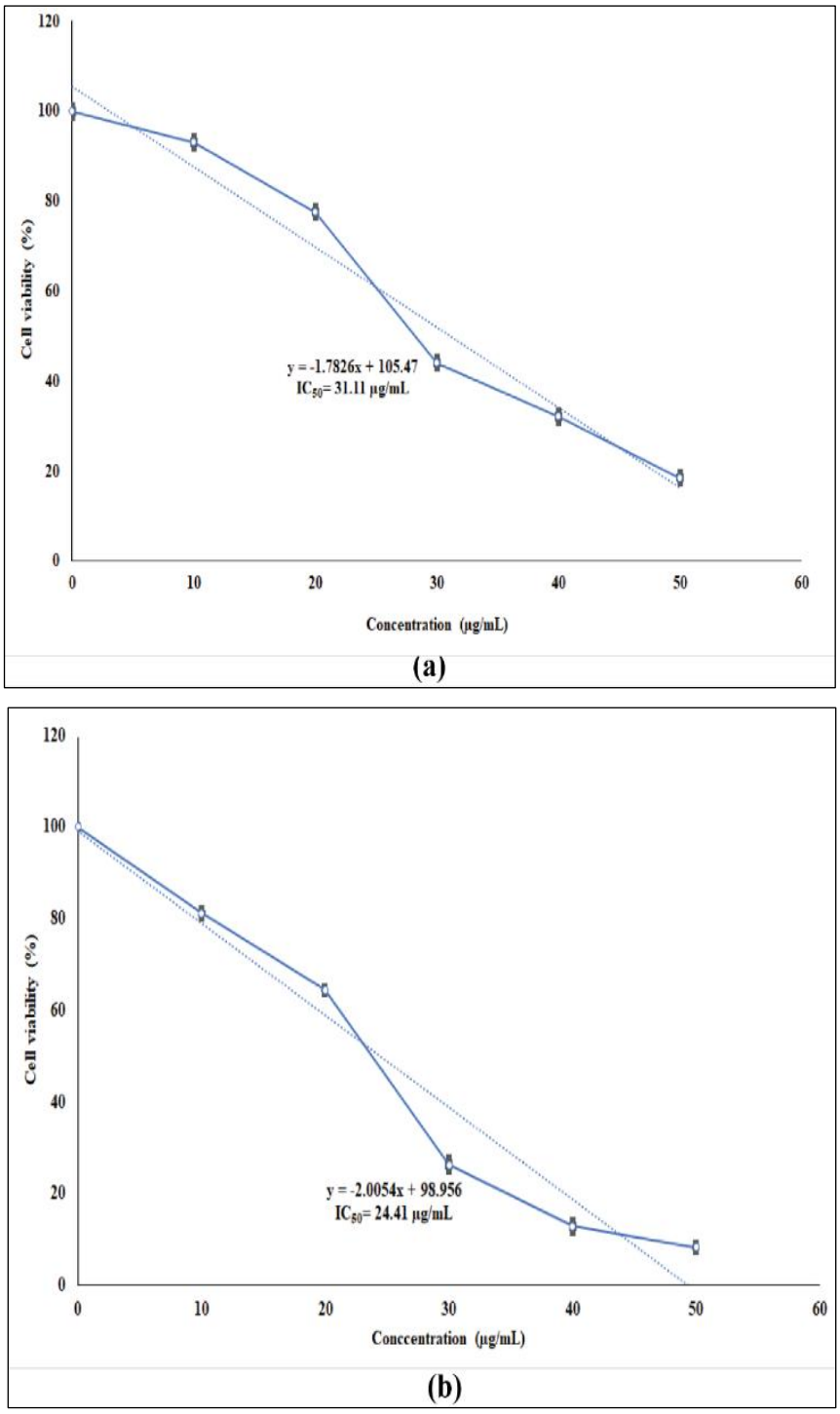


**Figure 11.** Graphical presentation of $IC_{50}$ concentration on HepG2 cell line by MTT assay **a)** CNH-SeNP **b)** CNH-SeNC

The CNH-SeNP were combined with PEG to synthesise *Cocos nucifera* haustorium selenium nanocomposite (CNH-SeNC). A conjugation of nanoparticles with a PEG enhances the pharmaceutical property by improving their bio-availability and permeability through cell membranes [33].

This was followed by characterising CNH-SeNP and CNH-SeNC through UV-visible, XRD, SEM-EDX and FTIR. The UV-visible result shows absorption maximum peak at 315 nm and 305 nm, this indicates elemental selenium's presence. Similar results were obtained in a study where SeNP were prepared using *Citrus limon* and *Citrus paradisi,* the peaks were identified between 300 nm to 550 nm [34].

The functional groups such as alcohols and carbohydrates have been involved in the stabilising process during the preparation of CNH-SeNP and CNH-SeNC. The FTIR study shows the functional groups on the outer layer of nanomaterials [26, 27]. The spherical nature of CNH-SeNP was confirmed using scanning electron microscopy, which is in accordance with the previous study [35].

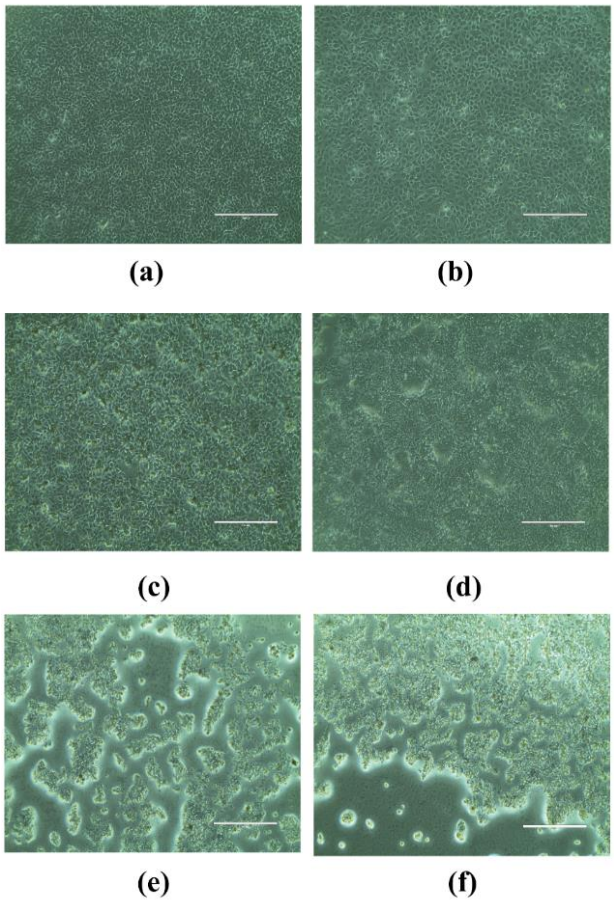


**Figure 12.** Structural changes in Vero and HepG2 cell line **a)** Vero cell line control **b)** Vero cell line treated with CNH-SeNP **c)** Vero cells treated with CNH-SeNC **d)** HepG2 control **e)** HepG2 treated with CNH-SeNP (IC50) **f)** HepG2 treated with CNH-SeNC (IC50). Images were taken at magnification 20X by phase contrast inverted microscope.

CNH-SeNC exhibited elongated oval morphology, with the size of CNH-SeNC being enlarged compared to CNH-SeNP after the coating of PEG, which is similar to the past study [15]. EDX analysis reveals the weight per cent of selenium in CNH-SeNP (5.6 %) and CNH-SeNC (13.0%). The result is in accordance with the work earlier work carried for ferulic acid-SeNPs, which showed the elemental content of C, O, Se and Na with 75 %, 16 %, 5 % and 2 % [36]. The amorphous form of the reducing agent would have masked the selenium [37].

The XRD depicts a clearly broad peak for CNH-SeNP, affirming its amorphous nature. This result is in coherence with the previously conducted study where fruit of *Emblica officinalis* were used to design SeNP, where the XRD study presented a broad peak indicating the amorphous form of SeNP [38]. The sharp XRD peaks reveal that the crystalline percentage has been increased in CNH-SeNC compared to CNH-SeNP, which may be due to the incorporation of PEG, which is confirmed by a peak at 23.62 degree, which is attributed to the XRD peak of PEG [39].

For the treatment of patients with chronic, long-lasting infections due to less immunity, it is significant to determine minimum bactericidal concentration and minimum fungicidal concentration. In this study, CNH-SeNP and CNH-SeNC have not shown considerable effect against pathogens taken into study. The size of the selenium nanoparticles plays role in the antimicrobial property of the nanomaterials [40]. The slightly lower antibacterial effect of CNH-SeNC compared to CNH-SeNP may be due to larger size of the fabricated selenium nanocomposites. Upon coating of PEG, the increased size of the selenium nanocomposites as well as the alterations on the surface of nanomaterials affects the interaction of nanocomposites with microbial membranes. The variations in the fabrication process and the reactants used influence the antimicrobial property [41, 42]. The maximum concentration of the CNH-SeNP and CNH-SeNC taken for the antimicrobial study was 100 µg/mL which might have not been sufficient to exhibit minimal inhibitory effect on the tested microbial strains. In some cases, the concentration of the nanomaterials to exhibit antimicrobial effect need to be higher than 100 µg/mL. In one of the previous studies, it was found that the MIC concentration of polymer coated SeNPs was 137 µg/mL and 274 µg/mL for *S. aureus* and *E. faecalis* which is greater than 100 µg/mL [43]. Another study, revealed that SeNPs were not efficient against *C. albicans*. In the same study, it was found that for some strains of *P. aeruginosa* the MIC was at 128, 256 and

512 µg/mL while for some strains of *P. aeruginosa* MIC was at lower concentration [44].

The sequestration of free radicals that cause severe damage to human health, inducing oxidative stress, is of prime importance. The antioxidant capacity of selenoproteins; selenocysteine catalyses the neutralisation of reactive oxygen species (ROS) to balance its level by removal of excess ROS [45] which supports the enhanced antioxidant effect of selenium. The antioxidant activity augmented with the increase in the concentration of CNH-SeNP and CNH-SeNC. In previous report, SeNP designed from *Emblica officinalis* fruit which comprised efficient antioxidative potential showed that 50% inhibition concentration of SeNP was lower than that of ascorbic acid through DPPH and ABTS assay [38]. In our study, ABTS showed higher scavenging properties among DPPH, ABTS, and $H_2O_2$ assays, which correlate with the previous findings [46]. CNH-SeNC has better antioxidant capacity than CNH-SeNP, may be due to antioxidant property of PEG [47] and other factors such as increased bio-availability. The property of antioxidation can be correlated to the stability of nanoparticles based on size, surface morphology and crystalline nature of the nanomaterials. Both CNH-SeNP and CNH-SeNC are well-dispersed which contributes to their efficient antioxidation property. From our study results we can infer that incorporation of PEG has increased the crystalline nature and size of CNH-SeNC compared to CNH-SeNP which attributes for the enhanced stability there-by improved antioxidation property of the selenium nanocomposite.

The results suggested that both CNH-SeNP and CNH-SeNC have better anti-inflammatory activities, as investigated through egg albumin denaturation and HRBC assays. For instance, in a study conducted using rats with inflammation, dosage of nano Se 2.55 mg/kg helped in lessening the inflammation induced in rats when given orally [48]. Therefore, a minimum concentration of CNH-SeNP and CNH-SeNC would be effective in treating inflammation. A study on rats proves that selenium nanoparticles can tune the damage caused by inflammation to liver cells by $CCl_4$ with its anti-inflammation potential [49]. In an earlier study, PEG coated *Gymnema sylvestre*-SeNPs with lupeol showed hemolysis of 12.8% which was almost twice 23.5% for uncoated *Gymnema sylvestre*-SeNPs with lupeol at 2 mg/mL. In similar way in the same study, at 2mg/mL PEG coated *Cinnamon cassia*-SeNPs with lupeol exhibited only 9.8% of hemolysis which was 18.9% for uncoated *Cinnamon cassia*-SeNPs with lupeol. The DPPH antioxidation capacity exhibited by PEG coated SeNPs of *Gymnema sylvestre* and *Cinnamon cassia* showed increased percentage of scavenging compared to free form of SeNPs [50]. This shows that the enhanced property of CNH-SeNC in HRBC assay and antioxidant property is attributed to the synergistic effect of selenium nanoparticles and PEG, which might lead to improved circulation time by incorporation of PEG.

PEG is a biocompatible polymer which can enhance the hemocompatibility of nanoparticles. This could have led to slightly increased hemocompatibility of CNH-SeNC compared to CNH-SeNP in our study. Biocompatible results achieved using the brine shrimp lethality test showed minimal toxicity at a higher concentration of the CNH-SeNP as well as CNH-SeNC. The lower concentrations were non-toxic. It was found that they are safe to use at lower concentrations, thus suggesting their compatibility is dosage-dependent and have to be used accordingly for biological applications [23].

The outcome of the anticancer studies on HepG2 cells indicated that apoptosis occurred due to CNH-SeNP, and CNH-SeNC is directly proportional to the concentration. According to the study carried using SeNP from *M. olifera*, the SeNP was potent in causing apoptosis with $IC_{50}$ as 150.87 µg (Caco-2), 392.57 µg (HepG2), 252.44 µg (MCF-7) [51]. The mode of action can be attributed to the ability of selenium nanoparticles and nanocomposites to generate reactive oxygen species (ROS) which in-turn creates oxidative stress in cancer cells. Additionally, coating of PEG prolongs the circulation time of selenium nanocomposites. The anti-oxidant property of selenium plays dual role; Selenium protects the normal cells form oxidative damage. While in cancer cells the excessive ROS formation triggers induction of apoptosis there-by inhibiting the growth of cancer cells. This shows the potent anti-cancer property of CNH-SeNP and CNH-SeNC while being biological compatible to normal cells.

The $IC_{50}$ value for CNH-SeNC was found to be 24.41 µg/mL which is lower compared to 31.11 µg/mL for CNH-SeNP proving the better efficiency of synthesised selenium nanocomposites over selenium nanoparticles. According to the earlier study, the PEG-SeNPs have greater inhibitory effect on R-HepG2 (Drug-resistance form of liver cancer cell line) with the rate of viability 14.8% at 16 µg/mL while the free form of SeNPs exhibited 88.9% at 12 µg/mL which was significantly lower in comparison to PEG-SeNPs thus proving the synergistic effect of PEG. $IC_{50}$ value showing anti-cancer effect was at 3.27 µg/mL for PEG-SeNPs showing the remarkable efficiency of the sample [52].

Hence, our research outcome reveals the bio-potential efficiency of *Cocos nucifera* haustorium-based selenium nanoparticles and nanocomposite infused with PEG on HepG2 cells. Besides, their effective anti-inflammatory property and bio-compatibility were also studied. Further investigations have to be carried out in the future to detail the *in-vitro* studies.

## 5. Conclusion

Fabrication of nanoparticles can be done using various species of plants, considering their disease-healing potency. The green synthesis technology encompasses the combination of plant's extract to salts

of selenium to design SeNP. In current research work, *Cocos nucifera* haustorium was used as a biological source to produce CNH-SeNP. The incorporation of PEG further enhanced the bioavailability and biomedical efficacy of selenium nanoparticles. Both CNH-SeNP and CNH-SeNC were characterised by various methods namely, UV-visible, XRD, SEM-EDX and FTIR. An investigation of their therapeutic effects was followed. It was found that they exhibit efficient antioxidative, anti-inflammation and anticancer potency. Besides, anticancer activity was studied in HepG2 cells, which showed that the cells were fragmented and got shrunk by the effect of CNH-SeNP and CNH-SeNC. It is predominantly seen that the synthesised nanomaterials from haustorium caused apoptosis in HepG2 cells without destroying the normal cells. Further, the findings from this investigation pay the way forward for the utilisation of plants in synthesising nanomaterials, which play a crucial role in combating human health. Henceforth, taking into consideration their potent pharmacological effect and bio-compatibility of CNH-SeNP and CNH-SeNC synthesised from haustorium of *Cocos nucifera,* they can be affirmed as a potential candidate in the stream of herbal based nano-medicines.

## 6. Future scope of the study

Our research outcomes revealed the remarkable *in vitro* results which can be further improved in the future by conducting in-depth studies that can provide insights to further understanding of the mechanism of action of CNH-SeNP and CNH-SeNC. In depth approach in future should focus on *in vivo* studies to validate the pharmaceutical property of CNH-SeNP and CNH-SeNC in biological systems. Furthermore, the mode of molecular mechanisms accounting for the antioxidant, anti-inflammatory, and anticancer activities need to be evaluated at the cellular and molecular levels. In addition, the potential of CNH-SeNP and CNH-SeNC in targeted drug delivery towards cancer cells can be analysed. These future approaches will pave the way for developing CNH-SeNP and CNH-SeNC as effective nano-formulations for multi-faceted therapeutic applications.

## References


[1] S. Khan, S. Mansoor, Z. Rafi, B. Kumari, A. Shoaib, M. Saeed, S. Alshehri,, M.M. Ghoneim, M. Rahamathulla, U. Hani, F. Shakeel, A review on nanotechnology: Properties, applications, and mechanistic insights of cellular uptake mechanisms. Journal of Molecular Liquids, 348, (2022). https://doi.org/10.1016/j.molliq.2021.118008

[2] V. Nayak, K.R. Singh, A.K. Singh, R.P. Singh, Potentialities of Se NPs in biomedical science. New Journal of Chemistry, 45(6), (2021) 2849-2878. https://doi.org/10.1039/D0NJ05884J

[3] N. Bisht, P. Phalswal, P.K. Khanna, Se NPs: A review on synthesis and biomedical applications. Materials Advances, 3(3), (2022) 1415-1431. https://doi.org/10.1039/D1MA00639H

[4] V. Alagesan, S. Venugopal, Green synthesis of selenium nanoparticle using leaves extract of Withania somnifera and its biological applications and photocatalytic activities. Bionanoscience, 9, (2019), 105-116. https://doi.org/10.1007/s12668-018-0566-8

[5] M. Govarthanan, Y.S. Seo, K.J. Lee, I.B. Jung, H.J. Ju, J.S. Kim, B.T. Oh, Low-cost and eco-friendly synthesis of silver NPs using coconut (Cocos nucifera) oil cake extract and its antibacterial activity. Artificial cells, nanomedicine, and biotechnology, 44(8), (2016) 1878-1882. https://doi.org/10.3109/21691401.2015.1111230

[6] M.M. Kumari, D. Philip, Facile one-pot synthesis of gold and silver nanocatalysts using edible coconut oil. Spectrochimica Acta Part A: Molecular and Biomolecular Spectroscopy, 111, (2013) 154-160. https://doi.org/10.1016/j.saa.2013.03.076

[7] A.H. Hashem, S.S. Salem, Green and ecofriendly biosynthesis of selenium nanoparticles using Urtica dioica (stinging nettle) leaf extract: Antimicrobial and anticancer activity. Biotechnology journal, 17(2), (2022) 2100432. https://doi.org/10.1002/biot.202100432

[8] S.K.R. Namasivayam, Eco friendly, green route method for the preparation of poly ethylene glycol (PEG) mediated surface modified iron oxide nanoparticles (PEG-IONps) with potential biological activities. Environmental Quality Management, 33(4), (2024) https://doi.org/10.1002/tqem.22172

[9] F. Liu, H. Liu, R. Liu, C. Xiao, X. Duan, D.J. McClements, X. Liu, Delivery of sesamol using polyethylene-glycol-functionalised Se NPs in human liver cells in culture. Journal of agricultural and food chemistry, 67(10), (2019) 2991-2998. https://doi.org/10.1021/acs.jafc.8b06924

[10] A. Narayanankutty, J.T. Job, A.M. Kuttithodi, A. Sasidharan, P.B. Benil, V. Ramesh, M.M.E. El-Din, M.F. Elsadek, H. Rizwana, Proximate composition, antioxidant, anti-inflammatory and antidiabetic properties of the haustorium from Coconut (Cocos nucifera L.) and Palmyra palm (Borassus flabellifer L.). Journal of King Saud University-Science, 35(1), (2023) 102404. https://doi.org/10.1016/j.jksus.2022.102404

[11] Y. Zhang, J. Kan, M. Tang, F. Song, N. Li, Y. Zhang, Chemical Composition, Nutritive Value, Volatile Profiles and Antioxidant Activity of Coconut (Cocos nucifera L.) Haustorium with Different Transverse Diameter. Foods, 11(7), (2022) 916.

https://doi.org/10.3390/foods11070916

[12] H. Omar, N.S.A. Malek, M.Z. Nurfazianawatie, N.F. Rosman, I. Bunyamin, S. Abdullah, Z. Khusaimi, M. Rusop, N.A. Asli, A review of synthesis graphene oxide from natural carbon-based coconut waste by Hummer's method. Materials Today: Proceedings, 75, (2022) 188-192. https://doi.org/10.1016/j.matpr.2022.11.427

[13] T. Liang, X. Qiu, X. Ye, Y. Liu, Z. Li, B. Tian, D. Yan, Biosynthesis of selenium nanoparticles and their effect on changes in urinary nanocrystallites in calcium oxalate stone formation. 3 Biotech, 10, (2020) 1-6. https://doi.org/10.1007/s13205-019-1999-7

[14] C. Santhosh, B. Balasubramanian, P. Vino, M. Viji, C. Rejeeth, S. Kannan, H. Ullah, K.R.R. Rengasamy, M. Daglia, M. Daglia, A. Maruthupandian, Biofabricated selenium nanoparticles mediated from Goniothalamus wightii gains biomedical applications and photocatalytic degrading ability. Journal of King Saud University-Science, 34(8), (2022) 102331. https://doi.org/10.1016/j.jksus.2022.102331

[15] C.O. Ehi-Eromosele, B.I. Ita, E.E.J. Iweala, The effect of polyethylene glycol (PEG) coating on the magneto-structural properties and colloidal stability of CO0. 8Mg0. 2Fe2O4 nanoparticles for potential biomedical applications. Digest Journal of Nanomaterials and Biostructures, 11, (2016) 7-14.

[16] S. Abirami, M. Priyalakshmi, A. Soundariya, A.V. Samrot, S. Saigeetha, R.R. Emilin, S. Dhiva, L. Inbathamizh, Antimicrobial activity, antiproliferative activity, amylase inhibitory activity and phytochemical analysis of ethanol extract of corn (Zea mays L.) silk. Current Research in Green and Sustainable Chemistry, 4, (2021) 100089. https://doi.org/10.1016/j.crgsc.2021.100089

[17] H.U. Hassan, N.I. Raja, F. Abasi, A. Mehmood, R. Qureshi, Z. Manzoor, M. Shahbaz, J. Proćków, Comparative study of antimicrobial and antioxidant potential of olea ferruginea fruit extract and its mediated selenium nanoparticles. Molecules, 27(16), (2022) 5194. https://doi.org/10.3390/molecules27165194

[18] M. Indracanti, S. ChV, T. Sisay, A 96 well-microtiter plate ABTS based assay for estimation of antioxidant activity in green leafy vegetables. Biotechnology International, 12 (2), (2019) 22-29.

[19] H. Sadiq, H. Sadiq, A. Sohail, A. Basit, N. Akhtar, K. Batool, S. Hisaindee, L. Asghar, Assessment of antioxidant activity of pure graphene oxide (GO) and composite V2O5/GO using DPPH radical and H2O2 scavenging assays. Journal of Sol-Gel Science and Technology, 108(3), (2023) 840-849. https://doi.org/10.1007/s10971-023-06231-6

[20] R. Shanmugam, M. Tharani, S.S. Abullais, S.R. Patil, M.I. Karobari, Black seed assisted synthesis, characterisation, free radical scavenging, antimicrobial and anti-inflammatory activity of iron oxide nanoparticles. BMC Complementary Medicine and Therapies, 24(1), (2024) 241. https://doi.org/10.1186/s12906-024-04552-9

[21] S. Sivakumar, M. Subban, R. Chinnasamy, K. Chinnaperumal, I. Nakouti, M.A. El-Sheikh, J.P. Shaik, Green synthesised silver nanoparticles using Andrographis macrobotrys Nees leaf extract and its potential to antibacterial, antioxidant, anti-inflammatory and lung cancer cells cytotoxicity effects. Inorganic Chemistry Communications, 153, (2023) 110787. https://doi.org/10.1016/j.inoche.2023.110787

[22] B.N. Meyer, N.R. Ferrigni, J.E. Putnam, L.B. Jacobsen, D.E.J. Nichols, J.L. McLaughlin, Brine shrimp: a convenient general bioassay for active plant constituents. Planta medica, 45(05), (1982) 31-34. http://dx.doi.org/10.1055/s-2007-971236

[23] D. Gopal, S. Partheeswar, T. Lakshmi, R. Shanmugam, Exploring the Therapeutic Potential: Green Synthesis of Selenium Nanoparticles Using Vaccinium Subg. Oxycoccus for Antioxidant, Anti-Inflammatory, and Cytotoxic Effect. Nanotechnology Perceptions, (2024) 632-648. https://doi.org/10.62441/nano-ntp.v20iS8.53

[24] T. Mosmann, Rapid colorimetric assay for cellular growth and survival: application to proliferation and cytotoxicity assays. Journal of immunological methods, 65, (1983) 55-63. https://doi.org/10.1016/0022-1759(83)90303-4

[25] D. Venkatachalapathy, C. Shivamallu, S.K. Prasad, G. Thangaraj Saradha, P. Rudrapathy, R.G. Amachawadi, S.S. Patil, A. Syed, A.M. Elgorban, A.H. Bahkali, S.P. Kollur, K.M. Basalingappa, Assessment of chemopreventive potential of the plant extracts against liver cancer using HepG2 cell line. Molecules, 26(15), (2021) 4593. https://doi.org/10.3390/molecules26154593

[26] M.M.R. Sreelekshmi, K.P. Sayoojya, A.P. Souparnika, K. Sowparnika, T.S. Pournami, K.R. Sabu, B.R. Rajesh, R.P. Chandran, Production of coconut sprout wine using Saccharomyces cerevisiae and its physico-chemical analysis. MOJ Food Process Technology, 6(5), (2018) 445-449. https://doi.org/10.15406/mojfpt.2018.06.00203

[27] J.A. Asong, E.K. Frimpong, H.A. Seepe, L. Katata-Seru, S.O. Amoo, A.O. Aremu, Green synthesis of characterised silver nanoparticle using cullen tomentosum and assessment of its antibacterial activity. Antibiotics, 12(2), (2023) 203. https://doi.org/10.3390/antibiotics12020203

[28] M. Smita, M. Bashir, S. Haripriya, Physicochemical and functional properties of

peeled and unpeeled coconut haustorium flours. Journal of Food Measurement and Characterization, 13(1), (2019) 61-69. https://doi.org/10.1007/s11694-018-9919-9

[29] R. Kizil, J. Irudayaraj, K. Seetharaman, Characterisation of irradiated starches by using FT-Raman and FTIR spectroscopy. Journal of agricultural and food chemistry, 50(14), (2002) 3912-3918. https://doi.org/10.1021/jf011652p

[30] Y. Xia, M. Sun, H. Huang, W.L. Jin, Drug repurposing for cancer therapy. Signal Transduction and Targeted Therapy, 9(1), (2024) 92. https://doi.org/10.1038/s41392-024-01808-1

[31] M. Soni, R. Gayathri, K. Sankaran, V.P. Veeraraghavan, A.P. Francis, Green synthesis of selenium nanoparticles using luffa cylindrica and its biocompatibility studies for potential biomedical applications. Nano, 18(06), (2023) 2350042. https://doi.org/10.1142/S179329202350042X

[32] M. Shahbaz, A. Akram, N.I. Raja, T. Mukhtar, A. Mehak, N. Fatima, M. Ajmal, K. Ali, N. Mustafa, F. Abasi, Antifungal activity of green synthesised selenium nanoparticles and their effect on physiological, biochemical, and antioxidant defense system of mango under mango malformation disease. PLoS One, 18(2), (2023) e0274679. https://doi.org/10.1371/journal.pone.0274679

[33] S.Y. Al-Qaraleh, W.A. Al-Zereini, S.A. Oran, A.Z. Al-Sarayreh, S.E.M. Al-Dalain, Evaluation of the antioxidant activities of green synthesised selenium nanoparticles and their conjugated polyethylene glycol (PEG) form in vivo. OpenNano, 8, (2022) 100109. https://doi.org/10.1016/j.onano.2022.100109

[34] G.B. Alvi, M.S. Iqbal, M.M.S. Ghaith, A. Haseeb, B. Ahmed, M.I. Qadir, Biogenic selenium nanoparticles (SeNPs) from citrus fruit have antibacterial activities. Scientific Reports, 11(1), (2021) 4811. https://doi.org/10.1038/s41598-021-84099-8

[35] L.M. Dos Santos Souza, M. Dibo, J.J.P. Sarmiento, A.B. Seabra, L.P. Medeiros, I.M. Lourenço, R.K.T. Kobayashi, G. Nakazato, Biosynthesis of selenium nanoparticles using combinations of plant extracts and their antibacterial activity. Current Research in Green and Sustainable Chemistry, 5, (2022) 100303. https://doi.org/10.1016/j.crgsc.2022.100303

[36] D. Cui, C. Yan, J. Miao, X. Zhang, J. Chen, L. Sun, L. Meng, T. Liang, Q. Li, Synthesis, characterization and antitumor properties of selenium nanoparticles coupling with ferulic acid. Materials Science and Engineering: C, 90, (2018) 104-112. https://doi.org/10.1016/j.msec.2018.04.048

[37] S.S. Salem, M.S.E. Badawy, A.A. Al-Askar, A.A. Arishi, F.M. Elkady, A.H. Hashem, Green biosynthesis of selenium nanoparticles using orange peel waste: Characterisation, antibacterial and antibiofilm activities against multidrug-resistant bacteria. Life, 12(6), (2022) 893. https://doi.org/10.3390/life12060893

[38] L. Gunti, R.S. Dass, N.K. Kalagatur, Phytofabrication of selenium nanoparticles from Emblica officinalis fruit extract and exploring its biopotential applications: antioxidant, antimicrobial, and biocompatibility. Frontiers in microbiology, 10, (2019) 931. https://doi.org/10.3389/fmicb.2019.00931

[39] G. Tien Nguyen, T.A.N. Truong, N. Duy Dat, T.A.D. Phan, T.H. Bui, Polyethylene Glycol Confined in SiO2–Modified Expanded Graphite as Novel Form–Stable Phase Change Materials for Thermal Energy Storage. ACS omega, 8(41), (2023) 38160-38169. https://doi.org/10.1021/acsomega.3c04311

[40] T. Huang, J.A. Holden, D.E. Heath, N.M. O'Brien-Simpson, A.J. O'Connor, Engineering highly effective antimicrobial selenium nanoparticles through control of particle size. Nanoscale, 11(31), (2019) 14937-14951. https://doi.org/10.1039/C9NR04424H

[41] A. Buzkova, L. Hochvaldova, R. Vecerova, T. Malina, M. Petr, J. Kaslik, L. Kvitek, M. Kolar, A. Panacek, R. Prucek, Selenium nanoparticles: influence of reduction agents on particle stability and antibacterial activity at biogenic concentrations. Nanoscale, (2025). https://doi.org/10.1039/D4NR05271D

[42] N. Filipovic, D. Usjak, M.T. Milenkovic, K. Zheng, L. Liverani, A.R. Boccaccini, M.M. Stevanovic, Comparative study of the antimicrobial activity of selenium nanoparticles with different surface chemistry and structure. Frontiers in bioengineering and biotechnology, 8, (2021) 624621. https://doi.org/10.3389/fbioe.2020.624621

[43] A. Rangrazi, H. Bagheri, K. Ghazvini, A. Boruziniat, M. Darroudi, Synthesis and antibacterial activity of colloidal selenium nanoparticles in chitosan solution: a new antibacterial agent. Materials Research Express, 6(12), (2020) 1250h3.

[44] E. Cremonini, E. Zonaro, M. Donini, S. Lampis, M. Boaretti, S. Dusi, P. Melotti, M.M. Lleo, G. Vallini, Biogenic selenium nanoparticles: characterization, antimicrobial activity and effects on human dendritic cells and fibroblasts. Microbial biotechnology, 9(6), (2016) 758-71. https://doi.org/10.1111/1751-7915.12374

[45] Y. Zhang, Y.J. Roh, S.J. Han, I. Park, H.M. Lee, Y.S. Ok, B.C. Lee, S.R. Lee, Role of selenoproteins in redox regulation of signalling and the antioxidant system: a review. Antioxidants, 9(5), (2020) 383. https://doi.org/10.3390/antiox9050383

[46] W. Chen, H. Cheng, W. Xia, Construction of Polygonatum sibiricum Polysaccharide Functionalized Selenium Nanoparticles for the Enhancement of Stability and Antioxidant Activity. Antioxidants, 11(2), (2022) 240. https://doi.org/10.3390/antiox11020240

[47] K. Juarez-Moreno, M. Ayala, R. Vazquez-Duhalt, Antioxidant capacity of poly (ethylene glycol) (PEG) as protection mechanism against hydrogen peroxide inactivation of peroxidases. Applied biochemistry and biotechnology, 177, (2015) 1364-1373. https://doi.org/10.1007/s12010-015-1820-y

[48] M.A. El-Ghazaly, N. Fadel, E. Rashed, A. El-Batal, S.A. Kenawy, Anti-inflammatory effect of selenium nanoparticles on the inflammation induced in irradiated rats. Canadian journal of physiology and pharmacology, 95(2), (2017) 101-110. https://doi.org/10.1139/cjpp-2016-0183

[49] H. Ebaid, J. Al-Tamimi, I. Hassan, M.A. Habila, A.M. Rady, I.M. Alhazza, A.M. Ahmed, Effect of selenium nanoparticles on carbon tetrachloride-induced hepatotoxicity in the Swiss albino rats. Applied Sciences, 11(7), (2021) 3044. https://doi.org/10.3390/app11073044

[50] S.B. Bi, I. Elahi, N. Sardar, O. Ghaffar, H. Ali, R.A. Alsubki, M.S. Iqbal, K.A. Attia, A.M. Abushady, Exploring non-cytotoxic, antioxidant, and anti-inflammatory properties of selenium nanoparticles synthesized from Gymnema sylvestre and Cinnamon cassia extracts for herbal nanomedicine. Microbial Pathogenesis, 192, (2024) 106670. https://doi.org/10.1016/j.micpath.2024.106670

[51] R. Hassanien, A.A. Abed-Elmageed, D.Z. Husein, Eco-friendly approach to synthesise selenium nanoparticles: Photocatalytic degradation of sunset yellow azo dye and anticancer activity. Chemistry Select, 4(31), (2019) 9018-9026. https://doi.org/10.1002/slct.201901267

[52] S. Zheng, X. Li, Y. Zhang, Q. Xie, Y.S. Wong, W. Zheng, T. Chen, PEG-nanolized ultrasmall selenium nanoparticles overcome drug resistance in hepatocellular carcinoma HepG2 cells through induction of mitochondria dysfunction. International journal of nanomedicine, (2012) 3939-3949. https://doi.org/10.2147/ijn.s30940

## Authors Contribution Statement

Y. Senthamaraikannan: Conceptualization, Methodology, Validation, Formal analysis, Investigation, Resources, Data curation, Writing- Original Draft, Writing- Review & Editing, Visualization, Supervision. V. Sundaram: Conceptualization, Methodology, Validation, Investigation, Resources, Writing- Review & Editing, Supervision, Project administration. R. Shanmugam: Conceptualization, Methodology, Validation, Investigation, Resources, Writing- Review & Editing, Project administration. All the authors read and approved the final version of the manuscript.

## Funding

The authors declare that no funds, grants or any other support were received during the preparation of this manuscript.

## Competing Interests

The authors declare that there are no conflicts of interest regarding the publication of this manuscript.

## Data Availability

The data supporting the findings of this study can be obtained from the corresponding author upon reasonable request.

## Has this article screened for similarity?

Yes

## About the License